International Journal of Heat and Mass Transfer 52 (2009) 3972–3983

Contents lists available at ScienceDirect

International Journal of Heat and Mass Transfer

journal homepage: www.elsevier.com/locate/ijhmt

Numerical study of flow patterns of compact plate-fin heat exchangers and generation of design data for offset and wavy fins

L. Sheik Ismail [a], C. Ranganayakulu [a], Ramesh K. Shah [b,*]

[a] Aeronautical Development Agency, PB No. 1718, Vimanapura Post, Bangalore 560017, India
[b] Energy Science and Engineering Department, IIT Bombay, Powai, Mumbai 400076, India

ARTICLE INFO

Article history:
Received 9 January 2009
Accepted 23 March 2009
Available online 3 June 2009

Keywords:
Numerical analysis
Offset strip fins
Wavy fins
Heat exchanger design data
Flow maldistribution

ABSTRACT

Thermo-hydraulic design of compact heat exchangers (CHEs) is strongly dependent upon the predicted/measured dimensionless performance (Colburn factor j and Fanning friction factor f vs. Reynolds number Re) of heat transfer surfaces. Also, air (gas) flow maldistribution in the headers, caused by the orientation of inlet and outlet nozzles in the heat exchanger, affects the exchanger performance. Three typical compact plate-fin heat exchangers have been analyzed using Fluent software for quantification of flow maldistribution effects with ideal and real cases. The headers have modified by providing suitable baffle plates for improvement in flow distribution. Three offset strip fin and 16 wavy fin geometries used in the compact plate-fin heat exchangers have also been analyzed numerically. The j and f vs. Re design data are generated using CFD analysis only for turbulent flow region. For the validation of the numerical analysis conducted in the present study, a rectangular fin geometry having same dimensions as that of the wavy fin has been analyzed. The results of the wavy fin have been compared with the analytical results of a rectangular fin and found good agreement. Similarly, the numerical results of offset strip fin are compared with the correlations available in the open literature and found good agreement with most of the earlier findings.

1. Introduction

Compact heat exchangers are widely used in aerospace, automobile and cryogenic industries due to their compactness (i.e., high heat transfer surface area-to-volume ratio) for desired thermal performance, resulting in reduced space, weight, support structure, footprint, energy requirement and cost. Depending on the application, various types of augmented heat transfer surfaces such as wavy fins, offset strip fins, louvered fins and perforated fins are used. They have a high degree of surface compactness and substantial heat transfer enhancement is obtained as a result of the periodic starting and development of laminar boundary layers over interrupted channels formed by the fins and their dissipation in the fin wakes. There is, of course, an associated increase in the pressure drop due to increased friction and form-drag contribution from the finite thickness of the interrupted fins. The surface geometries of wavy and OSF fins are described by the fin height (h), transverse spacing (s) and thickness (t). Interrupted flow length of the offset strip fin is described by offset strip/fin length (ℓ), and that of the wavy fin by the pitch of the wave (L).

Thermo-hydraulic design of a compact heat exchanger is strongly dependent upon the performance of heat transfer surfaces (in terms of Colburn factor j and Fanning friction factor f vs. Reynolds number Re characteristics). We focus here on offset strip fins and wavy fins. The orientation of inlet and outlet headers plays a major role in performance especially in aerospace applications, where the orientation of headers and nozzles are not straight and uniform due to space limitations. The effect of flow maldistribution on the exchanger performance is also investigated in this paper.

CFD analyses are conducted here for three different types of heat exchanger fin geometries in order to study the effect of flow maldistribution on the performance. For this purpose, design data in terms of j and f vs. Re for three different geometries of offset strip fins and 16 different geometries of wavy fins are derived numerically using CFD and presented in the form of j and f vs. Re curves. One of the rectangular fins has been analyzed and results are compared with Shah and London [10] analytical data for validation of numerical analysis. In addition, some of the offset strip fin correlations available in the literature are compared with Fluent results. Finally, the minimum qualification tests required for military airworthiness clearance are highlighted for these heat exchangers.

2. Literature review

The flow nonuniformity effects have been well recognized and presented for heat exchangers. Based on the literature by Shah and Sekulií [1], it has been understood that flow maldistribution

* Corresponding author. Mobile: +91 9448909152; fax: +91 80 25235992.
E-mail addresses: lsi786@yahoo.com (L. Sheik Ismail), rkshah@gmail.com (R.K. Shah).

0017-9310/$ - see front matter © 2009 Elsevier Ltd. All rights reserved.
doi:10.1016/j.ijheatmasstransfer.2009.03.026

Nomenclature

A	wave amplitude, mm
A_c	cross-sectional (flow) area, mm^2
A_f	total fin area on one fluid side, mm^2
A	total heat transfer area (fin + primary), mm^2
d_h	hydraulic diameter, $(4A_c)/P$ for wavy fin, mm
d_h	hydraulic diameter, $\frac{2(s-t)\ell}{[(s+h)\ell+th]}$ for offset fin, mm
f	Fanning friction factor, dimensionless
fpi	fins per inch
h	fin height, mm
j	Colburn factor ($StPr^{2/3}$), dimensionless
ℓ	offset strip/fin length, mm
L	pitch of fin waviness, mm
NTU	number of transfer units, dimensionless
P	perimeter, mm
Pr	Prandtl number, dimensionless
$PFHE$	plate fin heat exchanger
R	wavy fin curvature radius (see Fig. 4c), mm; $R1$, $R2$ and $R3$; R = 1 mm, R = 2 mm and R = 3 mm
r_h	hydraulic radius, mm
R_{max}	maximum radius, mm
Re	Reynolds number = $(\rho v d_h)/\mu$, dimensionless
$Rect$	rectangular fin
s	fin spacing, mm
S_ϕ	source term
St	Stanton number, dimensionless
t	fin thickness, mm
T_i	inlet temperature on hot fluid side, °C
T_o	outlet temperature on hot fluid side, °C
T	constant wall temperature, °C
v	flow velocity, m/s
Y^+	$(\Delta y_p v)\sqrt{\tau w/\rho}$, dimensionless

Greek symbols

α	s/h, dimensionless
α^*	$(h-t)/(s-t)$, dimensionless
δ	t/l, dimensionless
δ^*	$t/4r_h$, dimensionless
Δy_p	the distance of near wall node to the solid surface, m
λ_w	wave length of the wavy fin, mm
ℓ^*	$\ell/4r_h$, dimensionless
μ	dynamic viscosity, Ns/m^2
γ	t/s, dimensionless
ρ	density of the air, kg/m^3
τ_w	wall shear stress, N/m^2
ϕ	generalized transport variable
κ	turbulent kinetic energy, m^2/s^2
ε	turbulent dissipation rate, m^2/s^3
Γ	effective diffusivity, m^2/s

is mainly due to heat exchanger geometry and heat exchanger operating conditions. A few studies related to experimental investigation on flow maldistribution in plate heat exchangers are reported in the literature in recent years. Lalot et al. [2] investigated the effect of flow nonuniformity on the performance of plate heat exchangers. They found the optimum location for a perforated grid in the inlet header and observed reverse flow with poor header configuration. Ranganayakulu et al. [3] and Ranganayakulu and Seetharamu [4] investigated the effect of two-dimensional nonuniform flow distribution at inlet on both hot and cold fluid sides of crossflow plate-fin heat exchangers using a finite element model. It was found that the performance deteriorations and variations in pressure drops are quite significant in some typical applications due to fluid flow nonuniformity.

Zhang et al. [5] proposed a two modified headers with a two-stage-distributing structure to reduce the flow nonuniformity. They proved that the fluid flow distribution in plate-fin heat exchangers is more uniform if the ratios of outlet and inlet equivalent diameters for both headers are equal. Anjun et al. [6] introduced the concept of second header installation. By experimentation, they proved that the performance of flow distribution in PFHE is effectively improved by the optimum design of the both header configurations. Ranganayakulu et al. [7] studied the effects of the fluid flow nonuniformity due to the improper header/nozzle configuration with the CFD tool for a typical stainless steel compact plate-fin heat exchanger. Wen et al. [8] have investigated flow characteristics of the flow field in the entrance of a plate-fin exchanger by means of Particle Image Velocimetry (PIV). Based on the experiments, they suggested that a punched baffle could effectively improve fluid flow distribution in the header.

London and Shah [9] discussed performance of strip-fin core due to the following four non-dimensional geometrical parameters: dimensionless fin thickness δ^*, aspect ratio of flow passage in one fin pitch α^*, fin surface area to total surface area on the fin side A_f/A, and dimensionless strip length ℓ^* of offset strip fin geometry. Higher δ^*, α^*, A_f/A ratios tend to make higher j and f factors, and when ℓ^* is higher, both the j and f factors will tend to be lower. Because of smaller hydraulic radius, the non-dimensional roughness characterization influences much in f vs. Re characteristics. Shah and London [10] provided laminar flow analytical results (Nu and f vs. Re for various aspect ratios) for rectangular ducts. Later, Webb and Joshi [11] presented analytical models to predict the heat transfer coefficients and friction factors of an offset strip-fin heat exchanger by idealizing a unit cell model. The model neglected the possible burrs on the fin ends and also the roughness on the top and bottom of the channel. Wieting [12] gave empirical correlations based on the work done by Kays and London [17]. While generating those correlations, he had taken two Reynolds number regimes, such as, primarily laminar ($Re \leqslant 1000$) and primarily turbulent ($Re \geqslant 2000$). Mochizuki and Yagi [13] attempted to find the effect of the strip length on the j and f factors using their experimental study. They concluded that the optimum strip length has to be selected to get maximum goodness factor (j/f) value. Manson [14] developed correlations to predict thermo-hydraulic performances of offset fins. He gave two different equations for laminar and turbulent regions. Whereas, Manglik and Bergles [15] provided a single correlation that was applicable for laminar and turbulent regions for offset fins. Maiti [16] attempted multiple regression analysis using the data of Kays and London [17] and in-house experimental test results to establish general correlations. He considered the fully developed laminar flow up to Re equal to 10,000 in his numerical analysis.

Xi and Shah [18] carried out the 2D and 3D numerical computations for the idealized OSF in the laminar and transition flow regions to investigate differences between numerical results and experimental data and showed excellent correlation with the experimental data except at the highest Reynolds number. DeJong et al. [19] carried out both experimental and numerical simulation to establish a correlation for j and f factors. They found variations between numerical and experimental work. The assumption of two-dimensionality and the neglect of entrance and exit effects in the present numerical simulation may have also contributed to this difference. On the other hand, at low Reynolds number, the Colburn factor j estimated by numerical work is twice larger than the experimental work; but at high Reynolds number, it is

possible to predict it within ±10% accuracy. This behavior might be due to differences in the imposed boundary condition of constant heat flux for the numerical simulations and constant fin temperature for the experiments.

For generation of j and f vs. Re data numerically, the entry effects into the fin play a predominant role. In order to overcome this difficulty, Patankar et al. [20] introduced the concept of periodic fully developed flow and heat transfer. The underlying concept was that for a constant property flow in a duct of constant cross section, the velocity and temperature distributions become independent of the streamwise coordinate at sufficiently large distances from the inlet. The other important boundary condition that played a predominant role was the wall boundary condition for thermal analysis. Ciofalo et al. [21] mentioned that the constant temperature boundary condition yielded lower j values compared to those for the constant heat flux boundary condition but agreed well with the experimental values. Beale [22] explored fluid flow and heat transfer in inline and staggered tube banks. Fully developed cross flow was assumed throughout. Both constant wall temperature and constant heat flux boundary conditions were considered. He compared with existing experimental and numerical data.

Zhang et al. [23] modeled low Reynolds number periodically developed airflow and heat transfer ($Pr = 0.7$) in uniform wall temperature sinusoidal wavy plate channels. Numerical results for a wide range of steady laminar flow ($10 \leqslant Re \leqslant 1000$) and duct geometry variations ($0.125 \leqslant 2A/\lambda_w \leqslant 0.5$ and $0.1 \leqslant s/2A \leqslant 3.0$) were presented. They concluded that peak performance was obtained with $1.0 \leqslant s/2A \leqslant 1.2$. On the other hand, for a low flow rates ($Re \approx 10$), a much larger fin waviness severity ($2A/\lambda_w > 0.5$) may be required, in order to achieve any significant enhancement. Metwally and Manglik [24] obtained the numerical solutions for laminar ($10 < Re < 1000$) incompressible, single phase, periodically developed, constant property, forced convection in sinusoidal corrugated plate channels maintained at uniform wall temperature. They observed that the plate surface corrugations essentially generated transverse vortices in their trough regions and this recirculation was seen to grow with increasing $4A/\lambda_w$, Re and Pr. They found that optimum performance (j/f) obtained for corrugation geometries in the range $0.3 \leqslant 4A/\lambda_w \leqslant 0.6$. In the non-swirl flow region, the enlarged surface area of the corrugated plate was responsible for enhancement.

Manglik et al. [25] provided a detailed understanding of the forced convection behavior in wavy plate-fin channels and the effect of fin density in the steady low Reynolds number region for air flows ($Pr = 0.7$). They observed that the wavy wall surface produced a secondary flow pattern in the trough regions. Its magnitude and spatial coverage increased with Reynolds number and $s/2A$ ratio. They further concluded that thermal performance with constant heat flux condition was higher than that with constant wall temperature condition.

3. Flow nonuniformity analysis

3.1. Physical model

Three typical real plate-fin heat exchangers as shown in Figs. 1–3 are analyzed using the Fluent software in order to study flow maldistribution effects. Type I heat exchanger, made up of stainless steel, is a crossflow heat exchanger with one pass on the cold air side and two passes on the hot air side. It has 31 layers on hot air side for each pass and 32 layers on cold air side. The second heat exchanger, named as Type II made up of aluminum, is a crossflow heat exchanger having single pass on both fluid sides. It has 14 and 15 layers respectively on hot and cold air sides. The third heat exchanger, named as Type III, is a simple crossflow heat exchanger having single passes on both fluid sides with 5 and 6 layers on hot fuel and cold air sides.

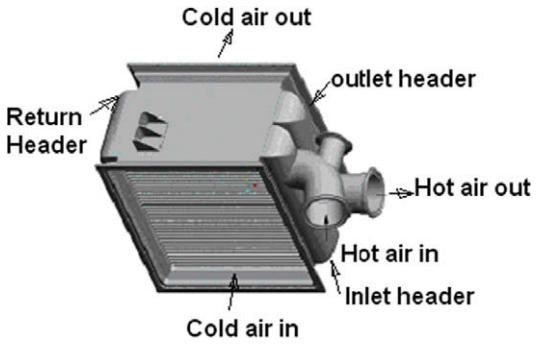

Fig. 1. Schematic of typical stainless steel heat exchanger (Type I).

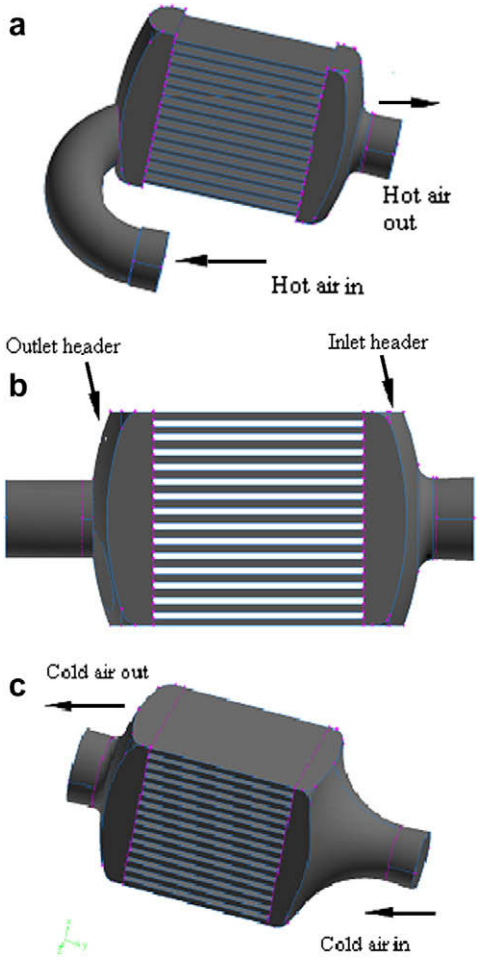

Fig. 2. Schematics of crossflow aluminum heat exchanger (Type II): (a) with hot air side fins and headers (real case), (b) with hot air side fins and headers (ideal case), and (c) with cold air side fins and headers (real/ideal case).

The above three plate-fin heat exchangers are manufactured with a combination of offset strip fins on the hot fluid side and wavy fins on the cold fluid side. Sketches of both types of fins are given in Fig. 4. Based on earlier studies by Ranganayakulu et al. [7,26,27], it is essential that proper header design is one of the solutions to reduce flow maldistribution and improve performance. They modified the header by placing a baffle plate in the inlet header and studied the effects of flow nonuniformity. The study of effects of entrance configuration on fluid flow maldistribution is

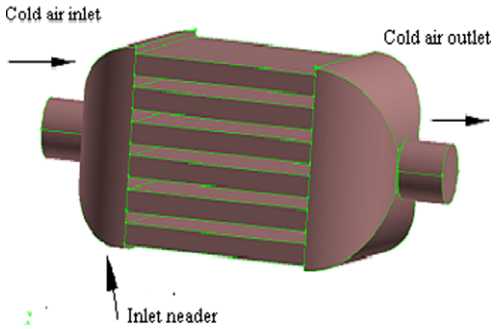

Fig. 3. Schematics of typical aluminum heat exchanger (Type III).

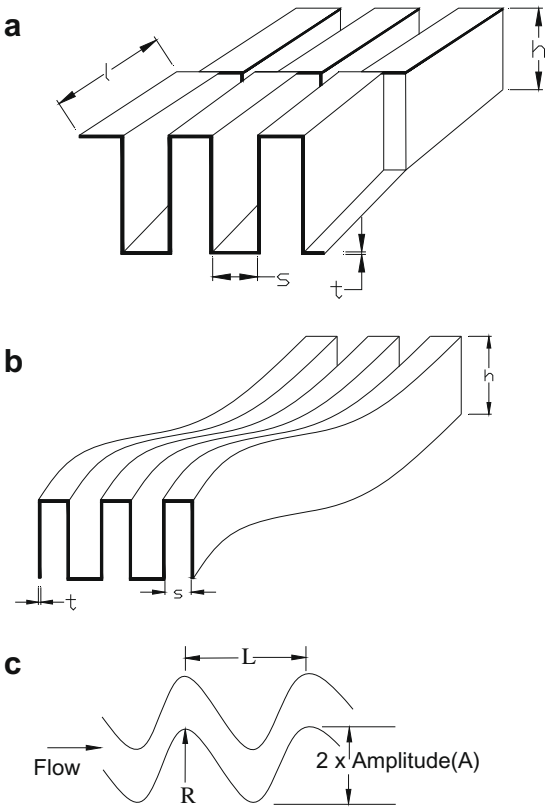

Fig. 4. Schematics of fin geometry: (a) offset strip fin, (b) wavy fin, and (c) wavy fin dimensional notations.

very important for optimizing the configuration and making the fluid flow more uniform in the heat exchanger. Thermo-hydraulic performances for the case (as shown in Fig. 1) with and without baffle plate at the inlet header are compared numerically to find out the variations in the flow distributions at the entry of the core.

Out of three heat exchangers, improvised header (modification of the header by placing the baffle) cases are analyzed for Types I and III heat exchangers. The typical improvised header configuration for Type I heat exchanger is shown in Fig. 5(a) and (b). The modified header shown in this figure is for the ideal case. It consists of a punched baffle plate placed at the distance of 85 mm from the inlet of the pipe to the header.

The baffle plate consists of a plate with varying dimensions of holes arranged such that the flow is made uniform throughout; otherwise most flow from the centered inlet pipe will go through the center region of the baffle plate. The holes at the center are small whereas the holes away from the center are bigger in diameter. A baffle plate with hole diameters of 10, 7 and 5 mm is shown in Fig. 5(b). As more flow is passing through the center of exchanger core when compared to sides/corners, 5 mm holes are selected for the center region of the baffle plate. Accordingly, hole diameters are increased to 7–10 mm in the peripheral regions of the baffle plate. These hole diameters are optimized by CFD such that more or less uniform flow enters the exchanger core. With the chosen hole pattern, the free flow area is reduced by 46.7%.

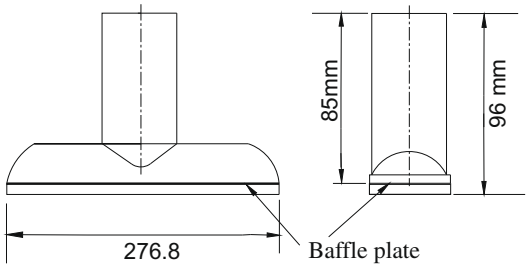

All dimensions are in mm

(a) Improvised header with a baffle

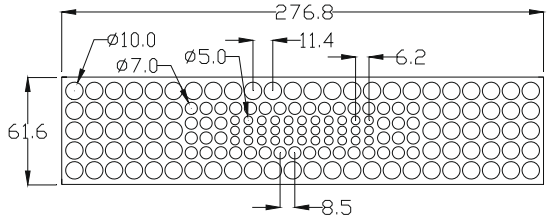

All dimensions are in mm

(b) Details of punched baffle plate

Fig. 5. Inlet header configuration of Type I heat exchanger.

The improvised header configuration for Type III heat exchanger is shown in Fig. 6a and 6b. It consists of a punched baffle plate which is placed at the distance of 46 mm from the inlet pipe as shown in Fig. 6(b). The thickness of the plate is 1 mm and the hole diameters are varied as 8 mm, 5.85 mm, 4.5 mm, 4 mm and 3.34 mm as shown in Fig. 6b. These hole diameters are optimized such that more or less uniform flow enters to the exchanger core. With the chosen hole pattern, the free flow area is reduced by about 50%.

3.2. Mathematical model

Following are some of the assumptions made in the CFD simulation: (a) the flow is stable in the computational domain; (b) the fluid flow meets the Boussinesq assumption and (c) the fluid in the domain is incompressible.

In this work, the CFD software Fluent is employed for simulation. In FLUENT, the conservation equations of mass, momentum and energy are solved using the finite volume method. There are several turbulence models available in the code. The turbulent flow is calculated by the semi-implicit SIMPLER as mentioned in Versteeg and Malalasekera [28] Algorithm method in the velocity and pressure conjugated problem, and a second order upwind differential scheme is applied for the approximation of the convection terms.

A standard κ–ε model as given in Versteeg and Malalasekera [28] with enhanced wall treatment is used to predict turbulent flow in the plate-fin heat exchanger as well as in the fin geometry. The Reynolds transport equations can be written in a generalized form as given in Ref. [29,30].

$$\mathrm{div}(\rho u\phi) = \mathrm{div}(\Gamma grad\ \phi) + S_\phi \quad (1)$$

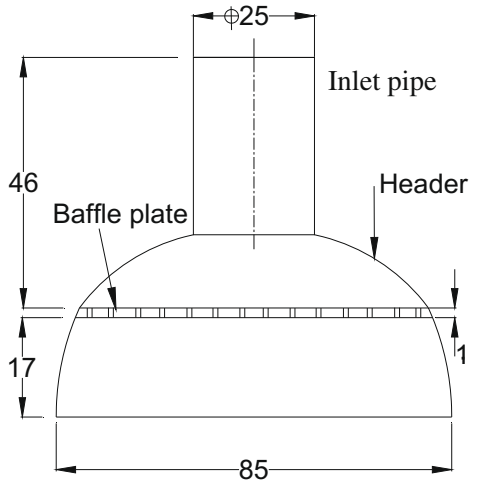

All dimensions are in mm

(a) Improvised header with a baffle

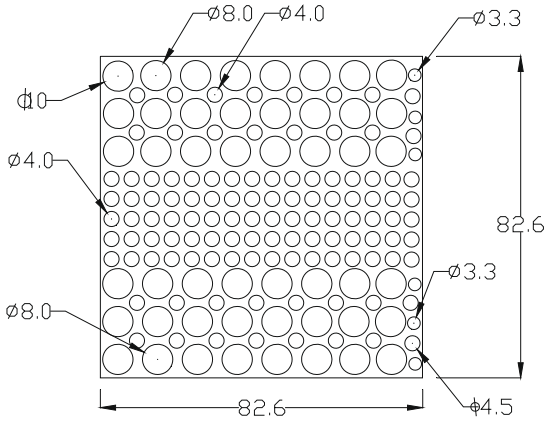

All dimensions are in mm

(b) Details of punched baffle plate

Fig. 6. Inlet header configuration of Type III heat exchanger.

where ϕ stands for a generalized transport variable, which is used for all conserved variables in a fluid flow problem, including, mass, momentum and the turbulence variables κ and ε. Γ represents the effective diffusivity (sum of the eddy diffusivity and the molecular diffusivity). S_ϕ is the source term for the respective dependent variable. The solution of the above set of equations is applied to the prediction of velocity and turbulence levels throughout the domain. The convergent criteria is specified to absolute residuals ($\leqslant 1.0 \times 10^{-5}$).

3.3. CFD approach

The entire CFD Analysis is carried out using the Fluent 6.2 in Red Hat Linux OS/HP xw8000 workstation with 2 GB RAM. In order to overcome the computational/software limitations due to the limitation on the mesh count and swap memory requirements of the workstation, the analysis is split into three phases. In Phase I, the heat exchanger core with the fins is replaced by porous medium as explained in Pantankar and Spalding [31] with appropriate equivalent core pressure drop to study the flow distribution. In the second phase, the fin that is used in the core is taken and characterized for f values over a range of Reynolds number. In third phase, the j value is determined for the same range by switching on the energy equation.

Both the heat exchangers (Type I heat exchanger shown in Fig. 1 and Type II heat exchanger shown in Fig. 2(a)) have bent pipes, which are not located at the center of the inlet headers. Hence, the flow to the matrix will be nonuniform even after replacing the fins with porous medium. Accordingly, the mass flow rate as the inlet boundary condition and pressure as outlet boundary condition have been given in the analysis of Phase I model. The results showed that there is flow nonuniformity in the entry of the core. The flow in the channels would become uniform if a suitable baffle plate were installed in the inlet header. For inlet maldistributed flow, there is no possibility of mixing of fluids within the channel of wavy fins.

Once the Phase I model of the heat exchanger is solved with the boundary conditions, the local mass flow rates are then determined at the entry of each channel and in turn the local Reynolds number, based on local flow velocity at entry of the exchanger core. In the Phase II model, a single layer of actual offset strip fin and wavy fin are modeled and meshed separately. Both the wavy fin and the offset strip fin are characterized over a range of Reynolds number to determine the corresponding j and f values. The fluid with nonuniform flow rates passes through the channels and enters the outlet header. Hence, we get different j and f values, in the channels of heat exchanger core, based on local flow rates. The mass flow rates are determined throughout the length of the core in different layers. In order to overcome the entrance effect, the concept of periodic fully developed flow as suggested by Patankar et al. [20] is implemented for this phase of flow analysis. After the analysis using Fluent, the pressure drop for unit length is one of the outputs, and that is multiplied by the actual length to get the total pressure drop for corresponding fins. From the pressure drop, friction factor is calculated as per Appendix A of Kays and London [17]. Finally, the corresponding two-dimensional fully developed velocity profile is listed out. Similarly, the same procedure is repeated for the range of Reynolds numbers from 2000 to 15,000 in order to draw the f vs. Re curves. Phase I and Phase II models are solved at quasi-isothermal condition to estimate the friction factors.

In Phase III model, the "velocity inlet" and "outflow" boundary conditions are used at the inlet and outlet of the fin geometry, respectively. The two-dimensional fully developed velocity profile, which is taken from the Phase II analysis (Pressure drop analysis), is used in the "velocity inlet" boundary condition. Constant wall temperature boundary condition is employed for walls as assumed in Maiti [16], Ciofalo et al. [21] and Beale [32]. Also, these approaches are basically explained in Spalding's PHOENICS code [33,34]. After the thermal analysis, post processing is done for temperatures and pressures at the inlet and outlet over the entire core length using mass weighted average, and pressure, temperature and velocity profiles are taken at the various sections of the fins for corresponding Reynolds numbers. This temperature difference between inlet and outlet of the core, in turn, is used for calculating j factor using Kays and London [17] methodology. Similarly, the same procedure is repeated for the range of Reynolds numbers from 2000 to 15,000 in order to draw the j vs. Re characteristic curves.

The geometry shown in Fig. 1 (Type I heat exchanger real case) meshed with 0.3327 million Hex-core hybrid elements (combination of hexagon and tetrahedral elements). The modified geometry is shown in Fig. 5. In some areas like headers, the pyramid elements are generated to connect hexagonal and tetrahedral elements. The actual mass flow rate, as shown in Table 1, is used as the boundary condition. No-slip boundary condition is used for walls.

The actual computation time taken for solving Phase I using 3D segregated k–ε turbulent model with enhanced wall treatment is 18 h. The time taken for solving Phase II using the same model is

Table 1
Heat exchangers experimental data.

Description	Flow (kg/s)	T_i (°C)	T_o (°C)	P_i (bar)	Pressure drop[a] (mbar)
Type I heat exchanger (hot side)	0.575	578	130	5.4	1890
Type I heat exchanger (cold side)	3.78	91.0	–	0.7	293.3
Type II heat exchanger (hot side)	0.575	107	95	10	216.7
Type II heat exchanger(cold side)	0.103	91.5	–	0.6	119.3
Type III heat exchanger (hot fuel side)	0.05	80	57.8	–	40
Type III heat exchanger (cold air side)	0.035	−9.3	61.5	–	44.1

[a] Total pressure drop including headers and nozzles.

26 h (the same time taken for characterization as stated in Phase III model). The solver took 15 h with initialization from Phase II model. The Type II heat exchanger is analyzed in the similar way for both hot and cold airsides. In this heat exchanger, both ideal and real cases are the same on the cold airside. But it is different for the hot air side. The ideal and real cases are shown in Fig. 2a and b. In the ideal case, the inlet pipe is made horizontal and aligned with axis of the heat exchanger and the pressure drop is determined. Since the velocity distribution in this heat exchanger is uniform because of smooth header configuration, improvised header cases are not considered for this heat exchanger analysis. Type III heat exchanger is also analyzed in the similar way for cold air side using porous media option. Subsequently, the k–ε turbulent codes with enhanced wall treatment are used for $Re \geqslant 2000$ for the generation of design data. The value of Y^+ is always maintained less than 3.

4. Validation of CFD data

The CFD data of Type I heat exchanger were validated with experimental data obtained in-house. In addition, a rectangular channel has been analyzed with CFD and compared with available published data in the following sub-sections. The results are found in good agreement in these comparisons.

4.1. Experimental data

Many assumptions have been made during the afore-mentioned numerical analysis. This may lead to uncertain results that may not be closer to experimental data. Hence, it is mandatory to conduct experiments for verifying the numerical analysis.

A compact heat exchanger test facility is available at Gas Turbine Research Establishment (GTRE), Bangalore. This test facility has Environmental Control System (ECS) test battery and provides a large range of airflow rate. Compressed air is supplied from the high mass flow rate facility to the process plant, which consists of a number of heaters and coolers, where the air is being processed to the required conditions and supplied to ECS test battery.

During experimental test trials of Types I–III heat exchangers at GTRE, the pressure drops and temperature drops were measured as listed in Table 1. The experimental pressure drop data (1890 mbar) of Type I heat exchanger can be comparable with CFD results (1866.6 mbar) as shown in Table 2. Similarly, the experimentation is carried out in steady state for Types II and III heat exchangers (including headers and nozzles) and its pressure drop values are presented in the same table.

4.2. Rectangular fin analysis

The analytical friction factors and heat transfer coefficients for the rectangular duct (fin) are already well established. A rectangular fin (the same as a rectangular duct considering fin efficiency as 100%) has been analyzed using CFD by considering uniform wall temperature boundary condition. Most of the authors like Zhang et al. [23], Metwally and Manglik [24] and Manglik et al. [25] who did extensive numerical work on wavy fins followed the same boundary condition. For the validation of the numerical analysis conducted in the present study, one of the rectangular fin having same dimensions (h, s, t) as that of the wavy fin has been analyzed in similar lines for the following fin: 10.2 mm fin height, 28 fins/inch (1.10 fins/mm) fin density and 0.152 mm fin thickness. In addition, a grid independence test is carried out for the same fin and a graph is plotted as the number of elements versus pressure drop as shown in Fig. 7(a). This figure shows that after 210,000 cells, there is not much variation in the pressure drop. The CFD results of rectangular fin are compared with Shah and London [10] results as shown in Fig. 7(b). In this figure, wavy fin data are also plotted for comparison. CFD results are in well accordance with the analytical results given by Shah and London [10] for the low Reynolds number region and the variations are found to be about 2% in j and 9% in f values.

4.3. Comparison with open literature

The results obtained from FLUENT (for fin 3.05S-28.5-0.0762) in the form of Colburn j and Fanning friction f factors are compared in

Table 2
Pressure drop of heat exchangers in break-up parts (refer to Fig. 1).

Heat exchanger	Description CFD/experimental results	Inlet to core	Core (1st pass)	Return header	Core (2nd pass)	Core to outlet	Total pressure drop
Type I (hot side) two pass	Real case (mbar)	178.1	578.6	76.5	590.6	456.8	1880.6
	Ideal case (mbar)	105.7	492.3	57.8	588.5	380.4	1624.7
	With baffle provided-real case inlet header (mbar)	175.3	492.3	58.0	588.5	323.8	1637.9
	Experimental data (mbar)	–	–	–	–	–	1890
Type II (hot side) single pass	Real case (mbar)	15.2	148.8	–	–	72.6	236.6
	Ideal case (mbar)	11.8	106.6	–	–	103.9	222.3
	Experimental data (mbar)	–	–	–	–	–	216.7
Type III (cold side) single pass	Real case (mbar)	1.01	13.28	–	–	18	32.29
	With baffle provided at the inlet header (mbar)	1.57	4.02	–	–	18.5	24.09
	Experimental data (mbar)	–	–	–	–	–	44.1

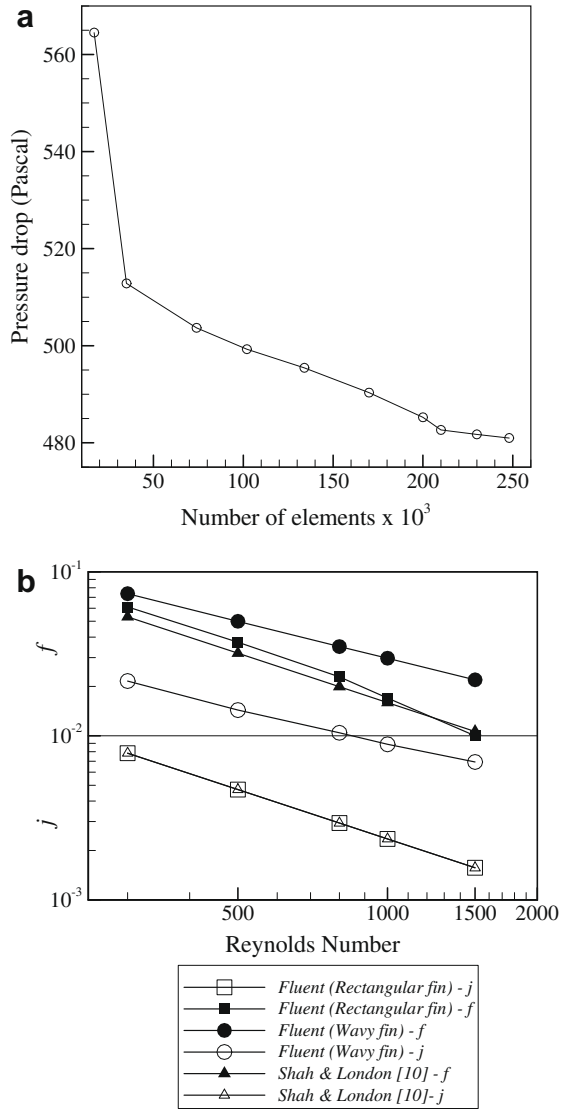

Fig. 7. (a) Grid independency graph. (b) Comparison of wavy and rectangular fin data.

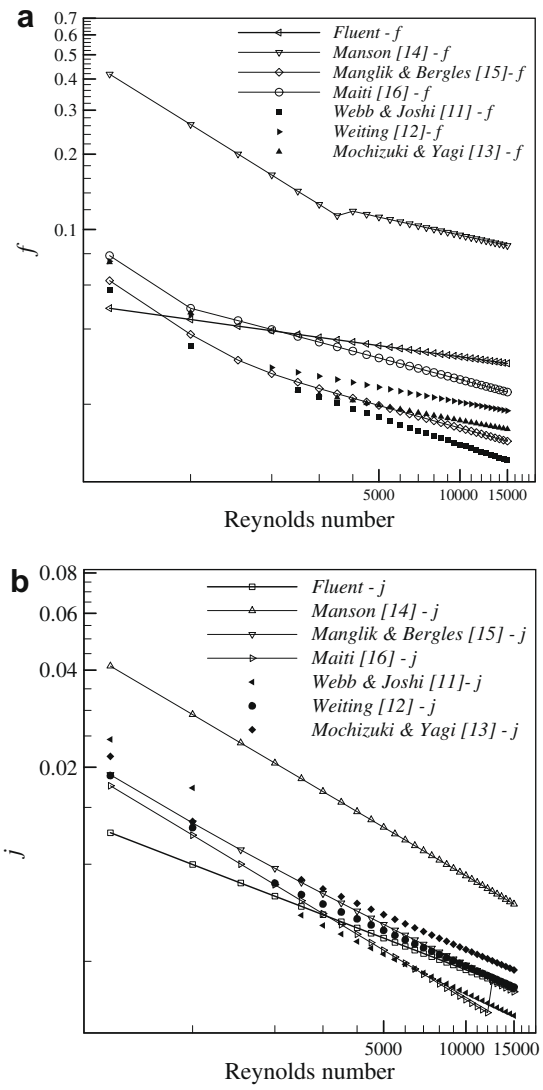

Fig. 8. Comparison of (a) "*f*" and (b) "*j*" factors with CFD Analysis for Fin (3.0S-28.5-0.0762).

Fig. 8a and 8b with the literature correlations. It is evident for *j* factors that only Wieting [12] and Manglik and Bergles [15] correlations are close to FLUENT results for high Reynolds numbers region.

Giving exact reasons for variation of these factors may not be possible due to involvement of so many parameters such as manufacturing aspects and testing conditions.

5. Results and discussion

The CFD results of heat exchangers with respect to flow nonuniformity are presented and possible ways were identified to eliminate it. The results obtained from Fluent for the stainless steel heat exchanger (Type I) in the form of Colburn factor *j* and Fanning friction *f* factor are compared with the improvised header (header with a baffle) configuration cases. The pressure drops for the real case and ideal case are compared in Table 2. There is an increase of about 256 mbar in the pressure drop that is about 16% higher in the real case when compared with the ideal case. This is because of inlet pipe location and orientation for Type I heat exchanger, as shown in Fig. 9. CFD analysis for heat transfer is carried out using Fluent with boundary conditions and respective mass flow rates in each layer of the fin. The local Reynolds numbers and corresponding *j* values are calculated. Then the average value of *j* factor is estimated using the mass weighted average as follows:

$$j_{\text{avg}} = \frac{\sum m_i j_i}{\sum m_i} \tag{2}$$

where *m* is the mass flow rate and *i* is the number of layers, which is 31 for Type I heat exchanger. Since flow is non-uniform in all 31 channels, the local *j* values are calculated first. Using the mass weighted average technique, the overall j_{avg} is calculated for the entire heat exchanger core and the value is found to be 0.006106. Similarly, the j_{avg} value obtained using the CFD for the ideal case without baffle is found to be 0.006056. However, the increase in *j* value, as compared to that for the ideal case, is almost negligible, when compared to the increase in the *f* factor. This is primarily because of more flow uniformity throughout all channels as compared to the ideal case, where the flow maldistribution is predominant. The pressure drop hike is nearly 13 mbar (about 1%) in the baffle plate case, when compared with the ideal case. The velocity profiles for the ideal and baffle plate cases are shown in the Figs. 10 and 11, respectively.

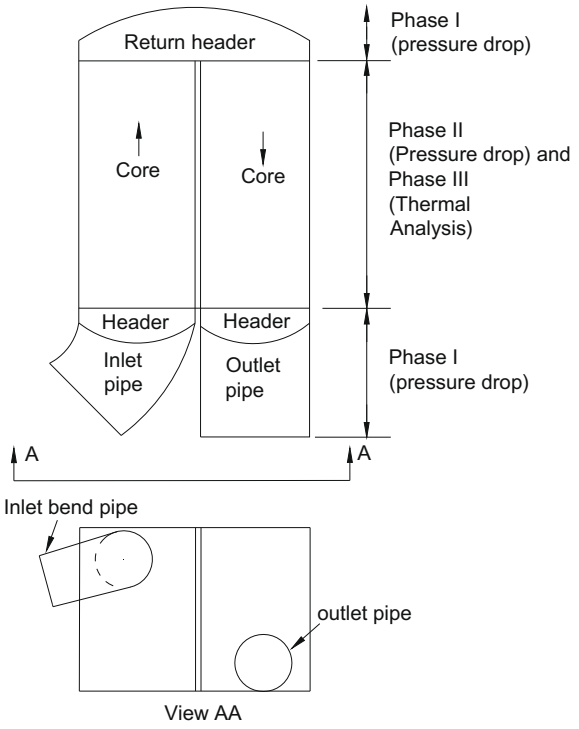

Fig. 9. Flow directions of Type I heat exchanger.

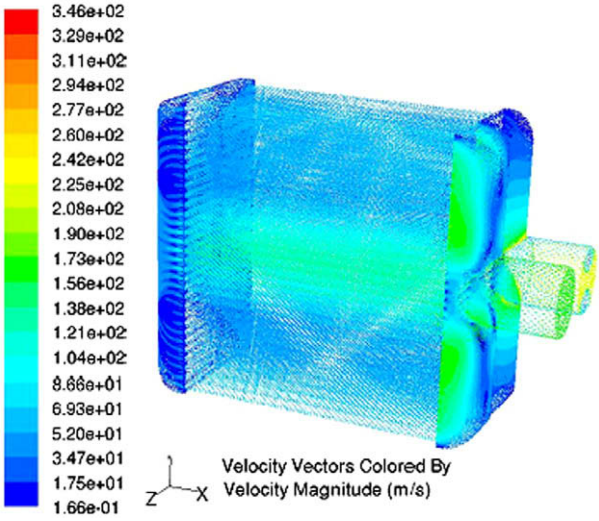

Fig. 10. Velocity distribution in ideal case of Type I heat exchanger.

Similarly, Types II and III heat exchangers are analyzed for flow nonuniformity effects. The breakdown of pressure drop results of the Type II hot air side and the Type III cold air side obtained from Fluent are compared with experimental data as shown in Table 2. The pressure drops for real and ideal cases are compared for hot air side of the Type II heat exchanger. It is observed that there is an increase of 14 mbar (about 6%) in the real case when compared with the ideal case. This is because of location/sharp bend at inlet pipe for Type II heat exchanger as shown in Fig. 2a. Similarly, the total pressure drop values for real/ideal and baffle plate cases of Type III heat exchanger (cold side) are compared and found that there is an increase of about 8.2 mbar (about 34%) in the real case when compared with the baffle plate case. The velocity distribution for Type II heat exchanger real case is shown in Fig. 12. Similarly, the velocity distributions for Type III real/ideal and baffle plate

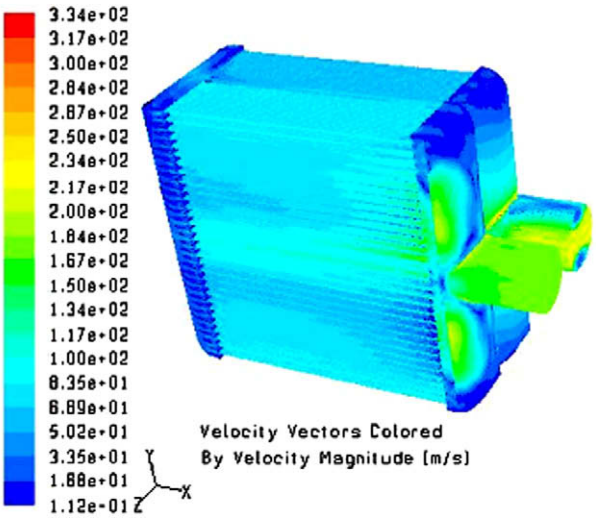

Fig. 11. Velocity distribution in baffle plate case of Type I heat exchanger.

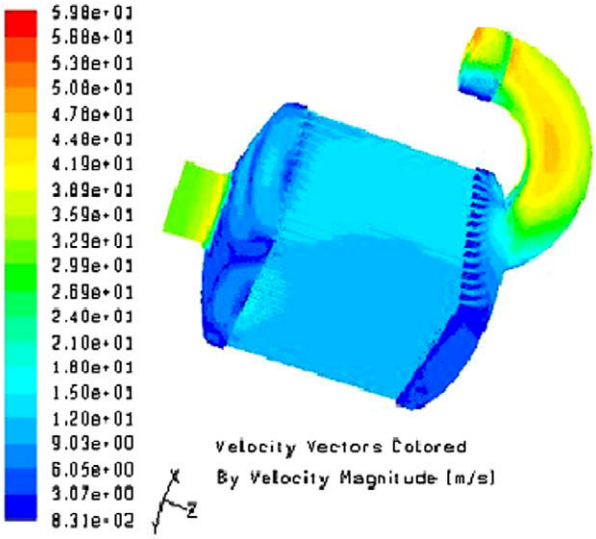

Fig. 12. Velocity distribution in the real case (hot air side) of Type II heat exchanger.

cases are shown in the Fig. 13a and b, respectively. These figures show that with the help of baffle plate, the flow uniformity can be improved to some extent.

Finally, the f and j values are generated using CFD technique for three types of offset strip fins and sixteen types of wavy fins. The computational domains and the velocity vector plots of both offset and wavy fins are shown in Figs. 14–17, respectively. The results are presented in Figs. 18–22 in the form of j and f vs. Reynolds number graph for the following fins:

Fin I: 2.54*H*-30-01016.
Fin II: 2.79*H*-18-0.152.
Fin III: 5.00*H*-28-0.076.
Fin IV: 10.2*L*-28-0.152 with *A*1.4 and *R*1.
Fin V: 10.2*L*-28-0.152 with *A*1.4 and *R*3.
Fin VI: 10.2*L*-28-0.152 with *A*1.4 and R_{max}.
Fin VII: 10.2*L*-28-0.152 with *A*1.7 and *R*1.
Fin VIII: 10.49*L*-11.44-0.152 with *A*2.0 [17].
Fin IX: 9.52*L*-11.5-0.254 with *A*2.0 [17].
Fin X: 10.49*L*-17.8-0.152 with *A*2.0 [17].

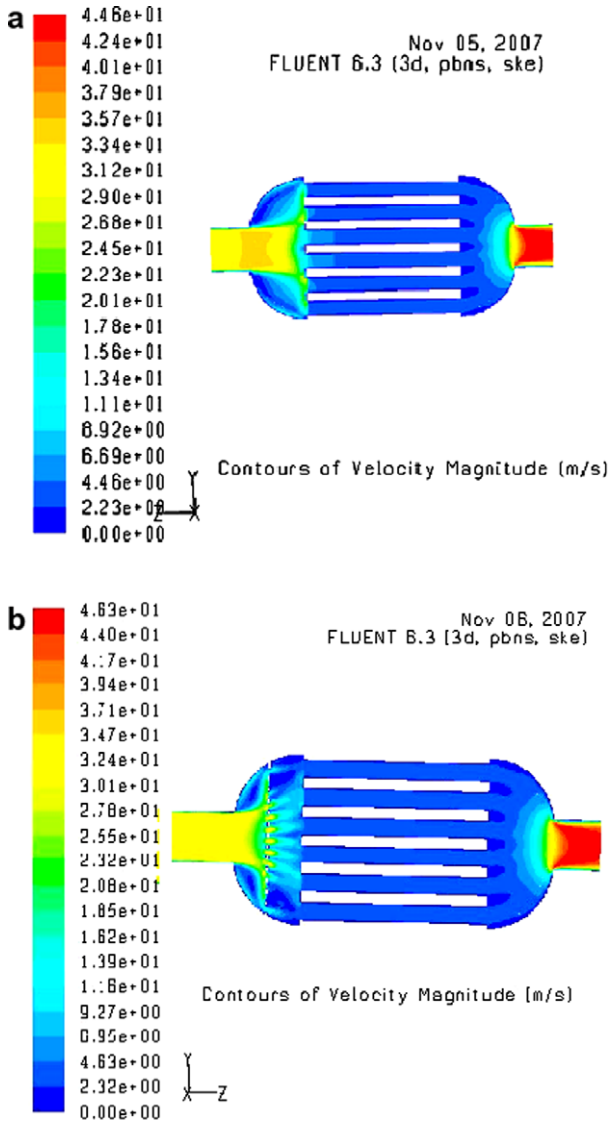

Fig. 13. Sectional view of velocity distribution of Type III heat exchanger (cold air side): (a) real/ideal case (b) baffle plate case.

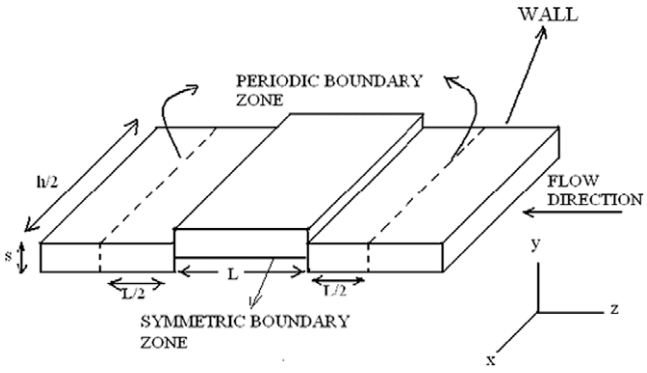

Fig. 14. Computational domain for an offset fin.

In the fin designation, the first number indicates the fin height. H and L denote the offset strip fin and the wavy fin, respectively. The second number indicates the fin density (fins/in) and the third number indicates the fin thickness.

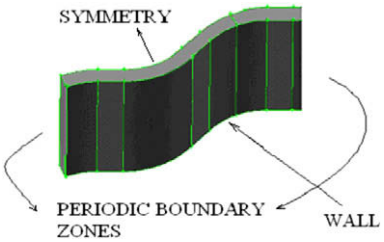

Fig. 15. Computational domain of a wavy fin.

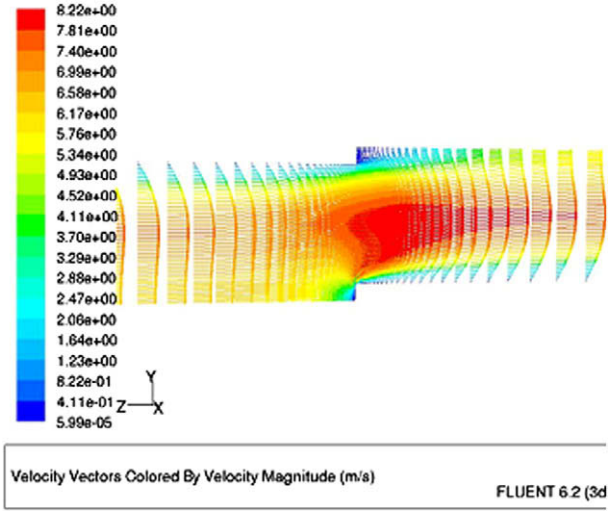

Fig. 16. Velocity vector plot at Reynolds number = 500 for Fin II.

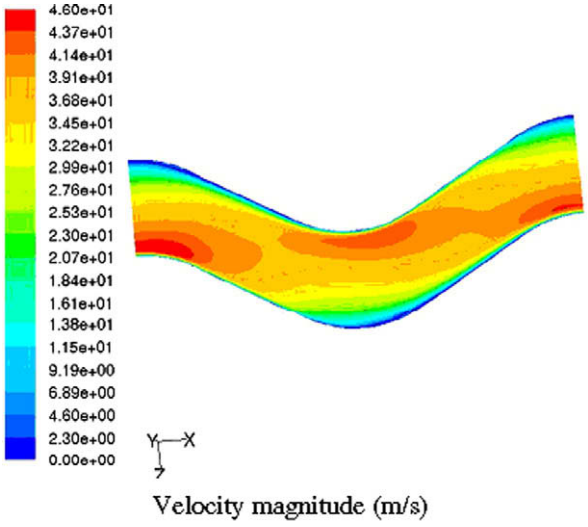

Fig. 17. Velocity magnitude plot at Reynolds number = 10,000 for Fin V.

From these graphs, it is observed that the j and f vs. Re curves of offset strip fins and wavy fins follow the same trends as Kays and London [17] experimental results of Figs. 10.60 and 10.75, respectively. The wavy fin dimensional details are shown in Fig. 4c. As the wavy fin amplitude A is increased from 1.4 to 1.7 mm, the friction factor is also increased. Also, it is observed that for a given wavy fin amplitude A and wavelength λ_w dimensions, the corner radius vary

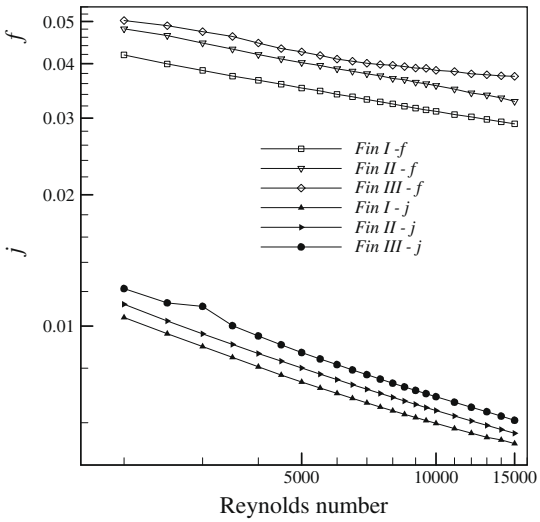

Fig. 18. Basic design data (j and f vs. Re) for offset strip fins.

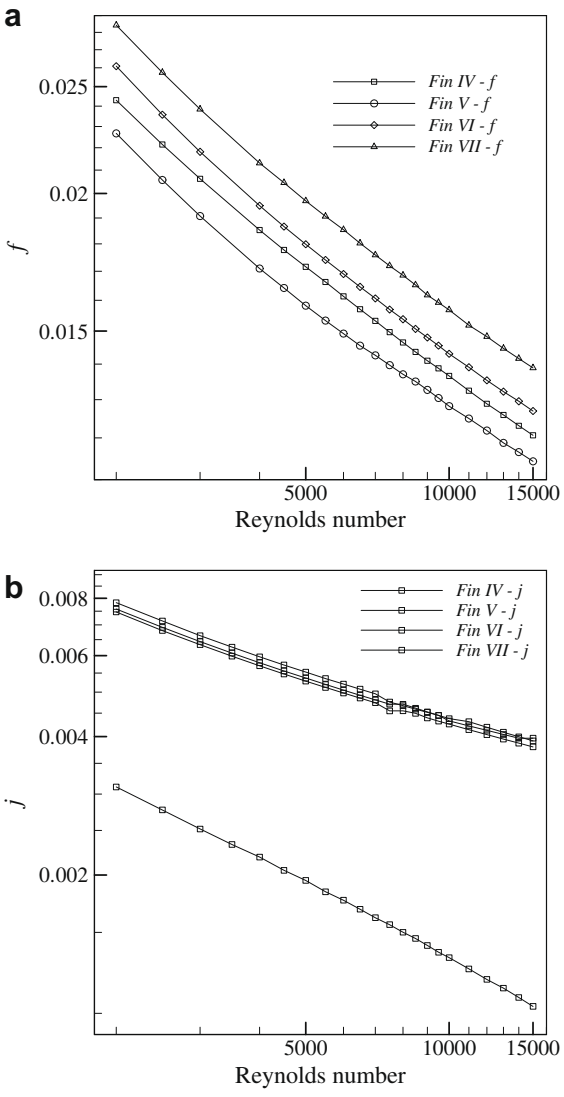

Fig. 19. Basic design data for wavy fins: (a) f vs. Re, and (b) j vs. Re.

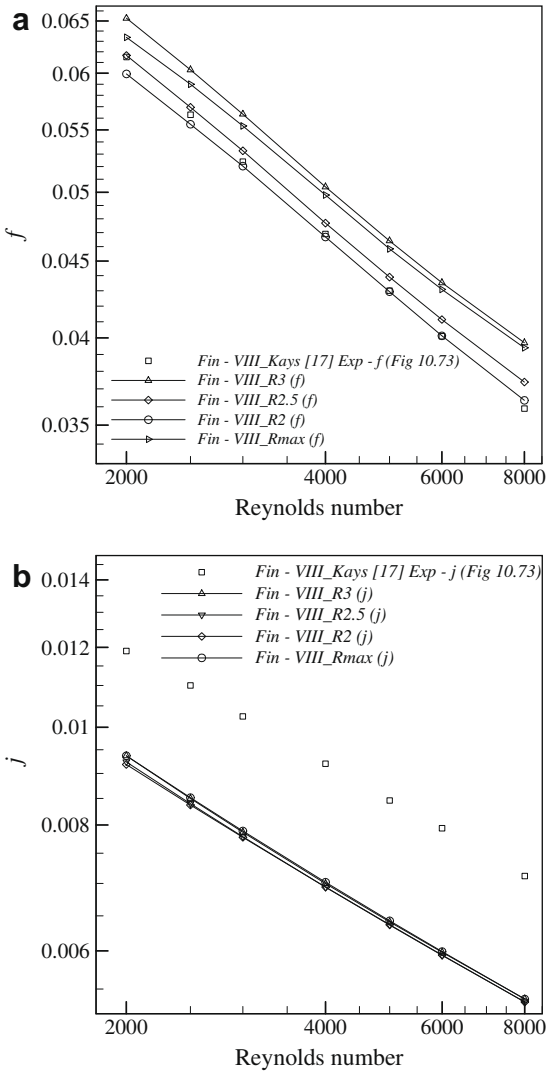

Fig. 20. Basic design data for wavy fins: (a) f vs. Re, and (b) j vs. Re.

from 1 to 4 mm (max) for wavy fins studied in this paper. These variations have significant effects on thermo-hydraulic performance as shown in Figs. 18–22. It has been observed that the Fin V with amplitude A of 1.4 mm and waviness radius R of 3 mm has 11–15% lower f values when compared with Fin VII, which has amplitude A of 1.7 mm and waviness radius R of 1 mm. In the case of thermal performance, Fin VII has the highest j value when compared with Fin IV, which is having amplitude A of 1.4 mm and waviness radius R of 1 mm. Similarly, it has been observed that the Fin VIII, Fin IX and Fin X with amplitude (A) 2 mm and maximum curvature radius have 2–8%, 15–27% and 17–20% higher f values, respectively, when compared with 2 mm corner radius R as shown in Figs. 20–22. Note that j values are higher for Fins VIII, IX and X with amplitude A of 2 mm and maximum curvature radius R. Further, the numerical results of Fins VIII, IX and X with different corner radii have been compared with Kays and London [17] (refer Fig. 10.73, 10.74 and 10.75), for which the curvature radius R is not known. From the results, it can be noted that the significant variations are observed in thermo-hydraulic performance due to difference in corner radius R. It is found that the wavy fin geometrical parameters (amplitude A and waviness radius R) play an important role in the performance. Hence, there is a need to choose an optimum corner radius R and amplitude A for improvement in performance.

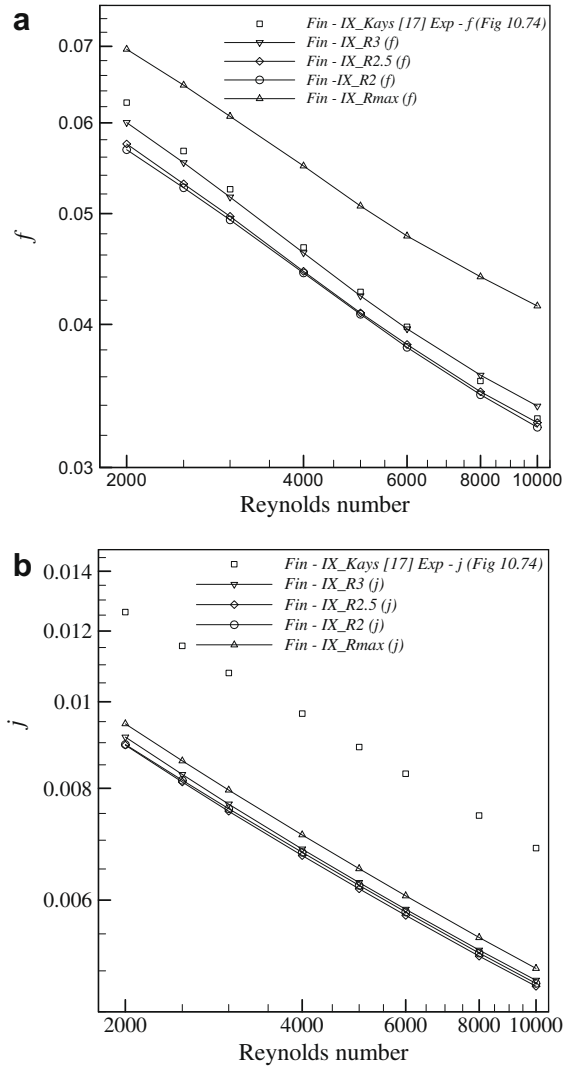

Fig. 21. Basic design data for wavy fins: (a) f vs. Re, and (b) j vs. Re.

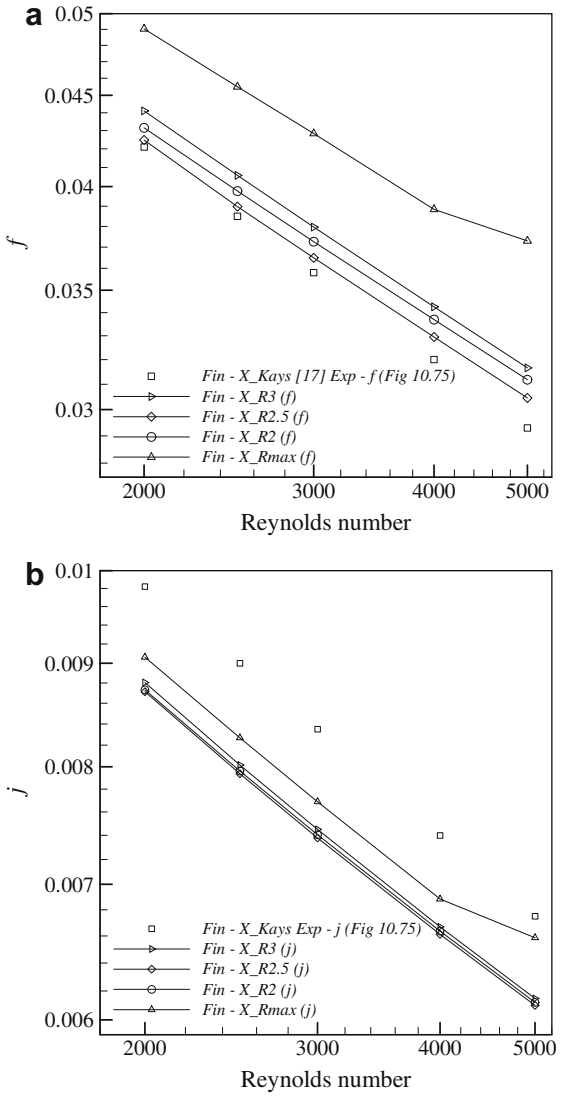

Fig. 22. Basic design data for wavy fins: (a) f vs. Re, and (b) j vs. Re.

6. Airworthiness aspects of heat exchangers

The above mentioned heat exchangers are subjected to different qualification tests as mentioned in Table 3 in order to asses the performance requirements and endurance life of heat exchangers for 3000 flying hours. Thermal Performance is carried out as per the design point test conditions given in Table 1 for these heat exchangers. In addition the structural integrity tests on these heat exchangers are carried out as per the test requirements given in MIL-STD-810E [35] and MIL-A-83116A [36].

Table 3
Qualification test for heat exchangers.

Sl. No.	Name of test	Mil specification
1	Acceptance tests	Basic dimensional check, leakage test, and pressure drop test
2	Thermal performance and pressure drop	Mil-A-83116A
3	Vibration	Mil-STD-810D
4	Pressure cycling	Mil-A-83116A
5	Thermal shock	Mil-A-83116A
6	Acceleration	Mil-STD-810D
7	Shock	Mil-STD-810D
8	Humidity	Mil-STD-810D
9	Fungus	Mil-STD-810D
10	Salt fog	Mil-STD-810D
11	Thermal performance and pressure drop	Mil-A-83116A
12	Combined pressure temperature and flow cycling	Mil-A-83116A
13	Burst pressure test	Mil-A-83116A

7. Conclusions

CFD analysis has been carried using Fluent software to study the flow patterns of compact plate-fin heat exchangers and design data generated for three types of offset fins and sixteen types of wavy fins. An extensive literature survey has been done on flow nonuniformity in the heat exchangers and possible ways to eliminate flow nonuniformity effects have been identified. The quantification of geometry-induced maldistribution has been reviewed in this paper. In order to estimate the geometry-induced maldistribution effects, three types of heat exchangers with and without baffle plate cases have been analyzed.

The pressure drop break up of stainless steel (Type I) heat exchanger has been calculated from Fluent data for both ideal and real cases. It has observed that the real case has about 16% higher pressure drop, when compared with the ideal case, which has a sharp bend at the heat exchanger inlet pipe. The Aluminum

(Type II) heat exchanger is analyzed for both ideal and real cases. The cold airside of the real case has about 6% higher pressure drop when compared to the ideal case due to the same reason as mentioned above. Further, since the header design in Type II heat exchanger has very smooth curvature, it has more or less uniform velocity distribution when compared with the Type I heat exchanger. This can be clearly seen from the velocity contours.

The Type III heat exchanger is analyzed for with and without baffle plate cases. The cold air in real case has about 34% higher pressure drop when compared to the baffle plate case. Subsequently, the new design data for three types of offset fins and 16 types of wavy fins have been generated using Fluent software version 6.2 and presented in the graphical form as j and f vs. Reynolds Number.

For the validation point of view, a rectangular fin having same dimensions as that of wavy fin has been analyzed using Fluent software and the characteristic curves have been compared with Shah and London [10] analytical data. It has been observed that both the curves have good agreement within ±2% in j and about ±9% in f values. In addition, results of one of the offset strip fins are compared with available correlations and found significant variations (see Fig. 8) in the thermo-hydraulic performance.

Acknowledgment

The authors acknowledge Aeronautical Development Agency, Bangalore, for allowing publishing this paper.

References

[1] R.K. Shah, D.P. Sekulić, Fundamentals of Heat Exchanger Design, John Wiley and Sons, New York, 2003, pp. 809–853.
[2] S. Lalot, P. Florent, S.K. Lang, A.E. Bergles, Flow maldistribution in heat exchangers, Int. J. Appl. Thermal Eng. 19 (1999) 847–863.
[3] Ch. Ranganayakulu, K.N. Seetharamu, K.V. Sreevatsan, The effects of inlet fluid flow nonuniformity on thermal performance and pressure drops in crossflow plate-fin heat exchangers, Int. J. Heat Mass Transfer 40 (1) (1997) 27–38.
[4] Ch. Ranganayakulu, K.N. Seetharamu, The combined effects of longitudinal heat conduction, flow nonuniformity and temperature nonuniformity in cross-flow plate-fin heat exchangers, Int. J. Comm. Heat Mass Transfer 26 (1999) 669–678.
[5] Z. Zhang, L. Yanzhong, CFD simulation on inlet configuration of plate-fin heat exchanger, Int. J. Cryogenic Eng. 43 (2003) 673–678.
[6] J. Anjun, R. Zhang, S. Jeong, Experimental investigation of header configuration on flow maldistribution in plate-fin heat exchanger, Int. J. Appl. Thermal Eng. 23 (2003) 1235–1246.
[7] Ch. Ranganayakulu, L. Sheik Ismail, C. Vengudupathi, Uncertainties in estimation of Colburn (j) factor and Fanning friction (f) factor for offset strip fin and wavy fin compact heat exchanger surfaces, in: S.C. Mishra, B.V.S.S.S. Prasad, S.V. Garimella (Eds.), Proceedings of the XVIII National and VII ISHMT – ASME Heat and Mass Transfer Conference, Guwahati, India, 2006, pp. 1096–1103.
[8] J. Wen, L. Yanzhong, A. Zhou, K. Zhang, An experimental and numerical investigation of flow patterns in the entrance of plate-fin heat exchanger, Int. J. Heat Mass Transfer 49 (2006) 1667–1678.
[9] A.L. London, R.K. Shah, Offset rectangular plate fin surfaces – heat transfer and flow friction characteristics, ASME J. Eng. Power 90 (Series A) (1968) 218–228.
[10] R.K. Shah, A.L. London, Laminar Forced Convection in Ducts, Supplement I to Advances in Heat Transfer, Academic Press, New York, NY, 1978.
[11] H.M. Joshi, R.L. Webb, Heat transfer and friction in the offset-strip fin heat exchangers, Int. J. Heat Mass Transfer 30 (1) (1987) 69–84.
[12] A.R. Wieting, Empirical correlations for heat transfer and flow friction characteristics of rectangular offset-fin plate-fin heat exchangers, ASME, Int. J. Heat Transfer 97 (1975) 480–490.
[13] S. Mochizuki, S. Yagi, Heat transfer and friction characteristics of strip fins, Int. J. Refrigeration 50 (1975) 36–59.
[14] S.V. Manson, Correlations of heat transfer data and of friction data for interrupted plate fins staggered in successive rows, NACA Tech. Note 2237, National Advisory Committee for Aeronautics, Washington, DC, 1950.
[15] R.M. Manglik, A.E. Bergles, Heat transfer and pressure drop correlations for the rectangular offset strip fin compact heat exchanger, Int. J. Exp. Thermal Fluid Sci. 10 (1995) 171–180.
[16] D.K. Maiti, Heat transfer and flow friction characteristics of plate-fin heat exchanger surfaces – a numerical study, PhD Thesis, IIT Kharagpur, India, 2002.
[17] W.M. Kays, A.L. London, Compact Heat Exchangers, Reprint Third Edition, Krieger Publishing, Malabar, FL, 1998; First Edition, Mcgraw Hill, New York, 1964.
[18] G. Xi, R.K Shah, Numerical analysis of offset strip fin heat transfer and flow friction characteristics, in: A. A. Mohamad, I. Sezai, (Eds.), Proceedings of the Computational Heat and Mass Transfer Conf., Eastern Mediterranean University Printing House, N. Cyprus, Turkey, 1999, pp. 75–87.
[19] N.C. DeJong, L.W. Zhang, A.M. Jacobi, S. Balachandar, D.K. Tafti, A complementary experimental and numerical study of the flow and heat transfer in offset strip-fin heat exchangers, ASME, Int. J. Heat Transfer 120 (1998) 690–698.
[20] S.V. Patankar, C.H. Liu, E.M. Sparrow, Fully developed flow and heat transfer in ducts having stream wise periodic variations of cross sectional area, ASME, Int. J. Heat Transfer 99 (1977) 80–186.
[21] M. Ciofalo, J. Stasiek, M.W. Collins, Investigation of flow and heat transfer in corrugated passages-II: numerical simulations, Int. J. Heat Mass Transfer 39 (1) (1996) 165–192.
[22] S.B. Beale, Fluid Flow and Heat Transfer in Tube Banks, PhD Thesis, Imperial College of Science, Technology and Medicine, London, 1993.
[23] J. Zhang, J. Kundu, R.M. Manglik, Effect of fin waviness and spacing on the lateral vortex structure and laminar heat transfer in wavy-plate-fin cores, Int. J. Heat Mass Transfer 47 (2004) 1719–1730.
[24] H.M. Metwally, R.M. Manglik, Enhanced heat transfer due to curvature-induced lateral vortices in laminar flows in sinusoidal corrugated-plate channels, Int. J. Heat Mass Transfer 47 (2004) 2283–2292.
[25] R.M. Manglik, J. Zhang, A. Muley, Low Reynolds number forced convection in three-dimensional wavy plate-fin compact channels: fin density effects, Int. J. Heat Mass Transfer 48 (2005) 439–1449.
[26] Ch. Ranganayakulu, L. Sheik Ismail, V. Vasudeva Rao, S. Rajeshwar, M. Ramu, Effects of Flow Maldistribution in a Compact Plate-Fin Heat Exchanger for Aerospace Applications – a CFD Approach, in: Proceedings of the 17th International Symposium on Transport Phenomena (ISTP17), Toyama, Japan, No. 2 C-III-3, 2006.
[27] Ch. Ranganayakulu, L. Sheik Ismail, R.K. Shah, Numerical study of flow patterns of compact plate-fin heat exchangers and generation of design data for offset and wavy fins, in: Ramesh K. Shah., Masaru Ishizuka., A.M. Jacobi, Viswas V. Wadekar. (Eds.), Proceedings of 6th International Conference on Enhanced, Compact and Ultra-Compact Heat Exchangers: Science, Engineering and Technology (CHE2007-0016), Germany, 2007, pp. 113–122.
[28] H.K. Versteeg, W. Malalasekera, An Introduction to Computational Fluid Dynamics, the Finite Volume Method, Prentice Hall, New York, 1995. pp. 62–146.
[29] John D. Anderson, Computational Fluid Dynamics, The Basic with Applications, McGraw-Hill Companies, Inc, New York, 1995.
[30] S.V. Patankar, Numerical heat transfer and fluid flow, Hemisphere, (1980) 79–86.
[31] S.V. Patankar, D.B. Spalding, A calculation procedure for the transient and steady-state behavior of shell-and-tube heat exchanger, in: N. Afgan, E.U. Schlunder (Eds.), Heat exchangers: Design and Theory Source book, Scripta Book Company, Washington, DC, 1974, pp. 156–176.
[32] S.B. Beale, Laminar fully developed flow and heat transfer in an offset rectangular plate-fin surface, PHOENICS, Int. J. Comput. Fluid Dyn. 3 (1) (1990) 1–19.
[33] D.B. Spalding, Four Lectures on the PHOENICS Code, Report, CFD/82/5, Computational Fluid Dynamics Unit, Imperial College, University of London, 1982.
[34] D.B. Spalding, PHOENICS 1984: A Multi-Dimensional Multi-Phase General-Purpose Computer Simulator for Fluid Flow, Heat Transfer and Combustion. Report, CFD/84/18, Computational Fluid Dynamics Unit, Imperial College, University of London, 1984.
[35] MIL-STD-810E, Environmental test methods and engineering guidelines, AMSC F4766, 1989.
[36] MIL-A-83116A, Air-conditioning sub system, air cycle, aircraft and aircraft launched missiles and general specifications, FSC 1660, London information (Rowse Muir) LTD, UK, 1971.